

On Closed-Shell Interactions, Polar Covalences, d Shell Holes, and Direct Images of Orbitals: The Case of Cuprite**

Shu-Guang Wang and W. H. Eugen Schwarz*

1. Introduction

During the last four decades of the previous century, efforts had been undertaken by “intellectual communities” (see, for example, Feyerabend^[1]) to surpass the “rational enlightenment” and the “critical rationalism” of Popper^[2] and others, though critiques of this epistemic relativism have never been silenced (for example, Sokal^[3]). The “postmodern” relativism had been prepared by Thomas Kuhn’s^[4] thesis that the historical development of science is a succession of incompatible viewpoints.

Fitting well into the popular “relativistic” convictions on differing viewpoints,^[1, 4] an experimental investigation on cuprite (Cu_2O) of combined X-ray and electron scattering has recently been interpreted^[5, 6a] regarding the four topics of this essay’s title. These authors “provide the first experimental verification of the controversial hypothesis that both ionic and covalent bonding occurs”^[5c] between copper and oxygen; they “demonstrate the existence of (covalent) bonding between pairs of copper”,^[5a, b] $\text{Cu}^+ \cdots \text{Cu}^+$, “with short metal–metal distances” of 3 Å,^[5a, c] which “is likely to make them re-write the chemistry textbooks”,^[5b] since “[X-ray diffraction is] unable to give details about the shape of the charge distribution”,^[6a] they claim “it is the first time that we have ever seen an orbital at this level of accuracy”,^[5c] namely “an unusual d-orbital hole”^[6a] in Cu^+ , and the “correspondence [between] the textbook d_{z^2} orbital is striking”.^[6a] These statements were enthusiastically presented during the last weeks of 1999 in many highly esteemed periodicals^[6] such as *Nature*, and *Chemical and Engineering News*^[6c] rated it among

the five most important chemical-research results of the last year. It seems to us necessary to refresh some textbook knowledge and we also include the results of some additional quantum-chemical calculations.^[7]

2. Polar Cu–O Bonding in Cuprite

Cuprite has received considerable interest because of it is a parent compound of the high temperature superconductors and of its interesting crystal structure.^[5, 8–11] Oxygen ions form a tetrahedral diamondlike lattice and a Cu^+ ion sits between each neighboring pair of O^{2-} ions to form the common linear $[\text{OCuO}]^{3-}$ dumb-bell unit. The Cu–O distance of 185 pm corresponds to the summation of the effective ionic radii^[12] of about 135 pm for O^{2-} (coordination number CN=4) and of about 50 pm for Cu^+ (CN=2). Because of the long O–O distances ($2 \times 185 = 370$ pm), this lattice has large holes, leaving enough space for a second, equivalent, interlacing lattice without requiring the lattices being explicitly bound together. The Cu^+ ions form a face-centered cubic lattice, that is, every unit cell contains eight Cu_4 tetrahedra each of volume $a^3/24$ (unit cell length $a = 427$ pm, $d(\text{Cu}–\text{Cu}) = 302$ pm), to leave four octahedral holes (volume = $a^3/6$) between them. One quarter of the Cu_4 tetrahedra is occupied by O atoms in the space group $Pn\bar{3}m$ (No. 224/2), while the other tetrahedra and all of the octahedra are empty.

Since the early development of quantum chemistry in the 1930s, the ideas of a partial charge transfer between ions and atoms, and of polar covalence between atoms of different electronegativity ($\chi_{\text{Cu}} = 1.8$; $\chi_{\text{O}} = 3.5$), have become adopted by the chemical community.^[13] Accordingly, effective charges of about $\text{Cu}^{0.5+}$ and $\text{O}^{1.0-}$ are expected. We have performed quantum chemical calculations of copper–oxygen structures (Figure 1) at the DFT (density functional theory) and SCF-MP2 levels of approximation, including relativistic corrections and using extended basis sets.^[7] We have found Mulliken and natural partial charges are $\text{Cu}^{(0.5 \pm 0.1)+}$ and $\text{O}^{(1.0 \pm 0.2)-}$.

Empirical electron-density determination by X-ray crystallography has become a mature field, exploiting synchrotron radiation and high-speed data collection devices, single crystal and powder diffraction, and electron and neutron scattering combined with theoretical techniques, a field competently reviewed in recent years.^[14, 15] Despite the point of view published in *Nature*,^[6a] Cu_2O has been the subject of several

[*] Prof. Dr. W. H. E. Schwarz, Dr. S.-G. Wang
Department of Chemistry
University of Siegen
57068 Siegen (Germany)
Fax: (+49) 271-740-2851
E-mail: schwarz@chemie.uni-siegen.de

[**] Discussions with Professors and Doctors G. von Büнау, B. Engelen, H. D. Lutz, J. Niu-Schwarz, and A. Pfützner (Siegen, Germany), R. Hoffmann (Ithaca, NY, USA), C. J. Humphreys (Cambridge, UK), A. Kirfel (Bonn, Germany), T. Lippman and J. Schneider (Hamburg, Germany), K. Schwarz (Vienna, Austria), M. Spackman (Armidale, Australia), J. C. H. Spence, M. O’Keefe and J. M. Zuo (Tempe AZ, USA), and financial support by Deutsche Forschungsgemeinschaft (DFG) and by Fonds der Chemischen Industrie (FCI) are all gratefully acknowledged.

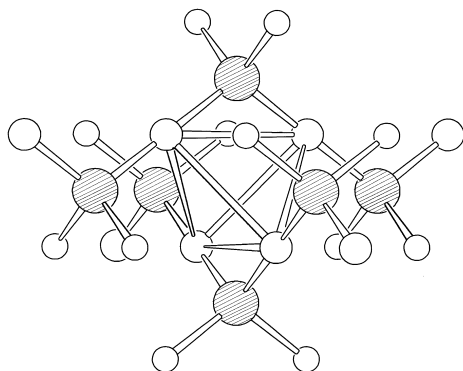


Figure 1. Copper–oxygen structures from the cuprite lattice. In the center lies the empty Cu_4 tetrahedron (smaller, open circles) at the $6d$ Wyckoff D_{2d} position, surrounded by six oxygen atoms (large, shaded circles). Every oxygen atom is surrounded tetrahedrally by four copper atoms. During calculation, variable numbers of the outer copper atoms were replaced by point charges in the range $[0, +\frac{1}{2}]$ in a symmetric manner to generate a neutral system.

experimental electron-density determinations,^[8–11] from which effective charges of $\text{Cu}^{(0.45–0.65)+}$ and $\text{O}^{(0.9–1.3)-}$ were deduced. The recent work^[5] is a good example of a state-of-the-art synergistic interaction of different techniques and of possible pitfalls. Remarkably, the effective charges reported therein ($\text{Cu}^{1.0+}$ and $\text{O}^{2.0-}$) differ significantly from the convergent collection of experimental and theoretical results.

3. The d Hole in $d^{10} \text{Cu}^+$ and the Effective Radius of Cu^+

In some of the literature on Cu_2O ,^[5, 9, 10, 16] it was mentioned that the Cu–O distance is short in comparison to the effective ionic radii. Similar comments can be found in the literature for some other compounds (see the discussion in ref. [17]). Such statements are often based on ionic radii which are either obsolete or the strong variation with coordination number had not been considered. The near-degeneracy of the nd and the $(n+1)s$ and $(n+1)p$ orbitals, and the linear symmetry of diagonally coordinated “coinage metal”(i) atoms are known^[16–19] to hybridize the nd_{z^2} and $(n+1)s$ orbitals to a σ -like orbital (Figure 2), and result in M^I ions with a slightly

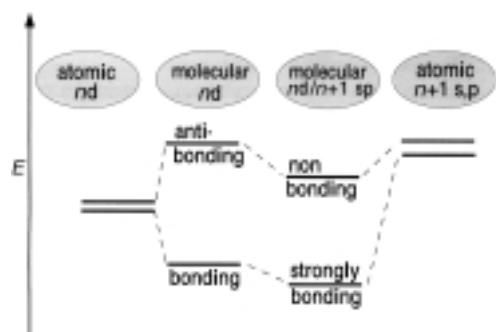


Figure 2. Schematic orbital energy diagram for atomic nd and $(n+1)s$, and molecular $d-d$ and $dsp-dsp$ orbitals.

oblate shape. All experimental and theoretical investigations of $[\text{XCuX}]^{3-}$ units ($\text{X} = \text{chalcogen}$) yield “short” internuclear distances, for example 185 pm for $[\text{OCuO}]^{3-}$.^[17, 19]

We have calculated^[7] the following natural atomic orbital (AO) populations on the “ $\text{Cu}^{0.5+}$ ” ion in Cu_2O as $d^{9.5}s^{0.75}p^{0.25}$. Zuo et al.^[5] reported $d^{9.8}s^{0.2}p^0$, that is, a less pronounced 3d hole and significantly less density in the 4sp shell. In either case, there is an electron deficiency in the formally closed 3d shell despite the 4sp electron excess on the (formally) singly charged copper ion. This was already well known from other experimental^[8–11] and theoretical investigations.^[16–19] The total electron density in Cu_2O and the differential electron density of Cu_2O with respect to Cu^{1+} and O^{2-} ions—the latter being stabilized in a positive lattice of point charges—are shown in Figures 3 to 5, where our SCF-MP2 results are compared with a common experimental $\Delta\rho$ map.^[5, 9–11]

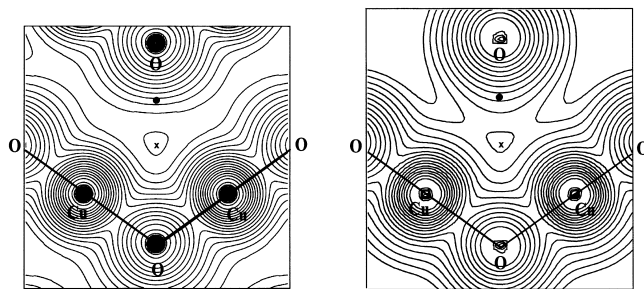


Figure 3. Total electron density in cuprite. Straight lines indicate the linear O–Cu–O units, and the dot (•) indicates the two copper atoms of the Cu_4 unit which lie above and below the plane. Contour line values are $0.05 \times 1.5^n \text{ e } \text{\AA}^{-3}$ ($n = 0, 1, 2, \dots$). Left: Experimental values of Lippmann and Schneider.^[11] Right: Our SCF-MP2 calculation. Note the similarity in the density minimum in the center (x) of the Cu_4 tetrahedra, which is at about $0.05 \text{ e } \text{\AA}^{-3}$ in the experiment and $0.07 \text{ e } \text{\AA}^{-3}$ in the calculation. Since the calculation refers to a cluster and not to an infinite crystal, the calculated electron density diminishes to zero outside.

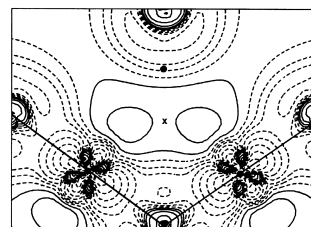


Figure 4. Calculated (SCF-MP2) difference electron density between cuprite (native cuprous oxide) and ions $\text{Cu}^+/\text{O}^{2-}$. Contour line values are $\pm 0.025 \times 2^n \text{ e } \text{\AA}^{-3}$ ($n = 0, 1, 2, \dots$); negative contours are dashed. Note the saddle point, rather than a maximum in the center of Cu_4 (*), $\Delta\rho < 0.05 \text{ e } \text{\AA}^{-3}$.

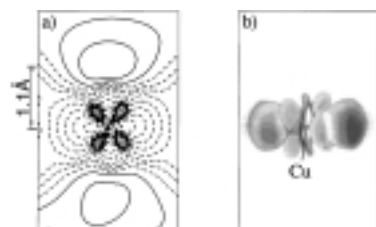


Figure 5. a) Calculated difference density around Cu in cuprite (see legend of figure 4). Note the d_σ hole on the horizontal axis the difference density of opposite, positive sign between the d_σ lobes, and the diffuse, extended positive lobes at the top and bottom (belt) due to d_σ -s hybridization. b) The respective computer graphic generated from ref. [5] without positive lobes above and below the horizontal axis.

4. Orbitals in “Nature”

In quantum mechanics, N -electron systems such as molecules or crystals are described by the many-electron wavefunction $\Psi(x_1, \dots, x_N)$, the density kernel $D(x_1, \dots, x_N, x'_1, \dots, x'_N)$ or, in the framework of DFT, by the single-particle probability $\rho(x_1)$, the so-called density. The x_i terms represent the canonical variables (position, momentum, angular momentum, and so forth) of one of the equivalent particles (electrons). The functions Ψ or D may (not necessarily must) be represented with the help of arbitrarily chosen single-electron orbitals φ_j . Within the ab initio approaches, the total density may then be represented by [Eq. (1)], where n_j is the occupation value of orbital φ_j . The orbitals are not all uniquely defined, only their sum is. In other words, orbitals represent arbitrary pieces of the total density (concerning some subtleties, see ref. [20]). Two points should be remembered:

$$\rho(r) = \sum_j n_j |\varphi_j(r)|^2 \quad (1)$$

Firstly, for some systems it is possible to choose the φ_j such that $n_j \approx 1$ for the first $j = 1 \dots N$ orbitals and $n_j \approx 0$ for the infinitely many other φ_j ($j > N$). In such cases the molecular orbital (MO) approximation is a reasonable approximation for many purposes [Eq. (2)]. For the DFT representation, there holds similarly for most systems [Eq. (3)], however, see ref. [21]. Now, let us compare two related N -electron systems a and b (for example, Cu_2O and $2\text{Cu}^+ + \text{O}^{2-}$). The so-called electron difference density is given in [Eq. (4)].

$$\rho(r) \approx \sum_j^N 1 \times |\varphi_j^{\text{MO}}(r)|^2 \quad (2)$$

$$\rho(r) = \sum_j^N 1 \times |\varphi_j^{\text{DFT}}(r)|^2 \quad (3)$$

$$\begin{aligned} \Delta\rho^{\text{ab}} &= \rho^{\text{a}} - \rho^{\text{b}} = \sum_j^N |\varphi_j^{\text{a,DFT}}|^2 - \sum_j^N |\varphi_j^{\text{b,DFT}}|^2 \\ &\approx \sum_j^N |\varphi_j^{\text{a,MO}}|^2 - \sum_j^N |\varphi_j^{\text{b,MO}}|^2 \end{aligned} \quad (4)$$

Secondly, often, orbital reorganization is small, which means that for all but few j , such as all j except $j = N$, $\varphi_j^{\text{a,DFT}} \approx \varphi_j^{\text{b,DFT}}$ and/or $\varphi_j^{\text{a,MO}} \approx \varphi_j^{\text{b,MO}}$. Then the electron difference density is given in [Eq. (5)]. The quantity $\Delta\rho^{\text{ab}}$

$$\Delta\rho^{\text{ab}} \approx |\varphi_N^{\text{a,DFT}}|^2 - |\varphi_N^{\text{b,DFT}}|^2 \approx |\varphi_N^{\text{a,MO}}|^2 - |\varphi_N^{\text{b,MO}}|^2 \quad (5)$$

represents the difference of two positive quantities and integrates to zero over the whole space; the positive and negative regions of the electron difference density cancel. If ionization is considered, either $\varphi_N^{\text{b,DFT}}$ or $\varphi_N^{\text{b,MO}}$ describe the ionized electron, which is distributed over the whole space with vanishing electron density everywhere and therefore [Eq. (6)] follows. The (not everywhere positive) differential

$$\Delta\rho^{\text{ion}} \approx |\varphi_N^{\text{a,MO}}|^2 \approx |\varphi_N^{\text{a,DFT}}|^2 \quad (6)$$

density $\Delta\rho^{\text{ion}}$ can often, but not always, be approximated by a single, everywhere positive, orbital density. If bonding in a

crystal is considered and one compares the experimentally investigated compound with the theoretically computed atoms or some selected ions, then $\varphi_N^{\text{b,MO}}$ or $\varphi_N^{\text{b,DFT}}$ is an atomic (ionic) orbital and $\varphi_N^{\text{a,MO}}$ or $\varphi_N^{\text{a,DEF}}$ is a localized Wannier orbital over the unit cell of the crystal. Then $\Delta\rho^{\text{bond}}$ is the difference of two localized charge distributions.

In summary, if the two systems compared can be well approximated by a finite number of appropriately chosen orbitals, and if most of these orbitals of the two systems can be chosen to be very similar, then the electron difference density of the two systems—for instance an experimentally investigated real one and a chosen theoretical reference—can be well approximated by the difference of the two chosen orbital densities. Thirdly, if furthermore one of these two orbitals is rather diffuse, then the difference density is dominated by the shape of the other orbital density map. Finally, and extending still further, if this orbital has large values on one atom only, $\Delta\rho$ is similar that of an atomic hybrid. This special situation does occur quite often for transition-metal compounds and a number of such cases, of levels of accuracy in the range of several $0.1 \text{ e } \text{\AA}^{-3}$ down to a very few $0.01 \text{ e } \text{\AA}^{-3}$, can be found in the literature.^[14, 15] An early experimental example, where the $\Delta\rho$ looked like “a textbook picture of a d atomic orbital”, was published in ref. [22], and one of the more recent ones is presented beautifully as a computer-generated graphic in *Nature*^[5] (Figure 5b). Such cases are correctly described not as an orbital in nature but as a case where one has found two systems for which conditions 1) to 4) could be fulfilled.

5. The Shape of Orbitals

Orbital densities $|\varphi|^2$ are real, positive functions in three-dimensional space. The respective orbital functions themselves may have positive or negative “phases” (or even complex phases in magnetic fields, or quaternionic phases^[23] in the case of relativistic spin-orbit coupling). These functions may be represented by contour surface graphics or in two dimensions by contour line maps. The contour lines or envelopes of an orbital cannot touch each other, because there exist regions of lower density and a zero surface between the lobes. These lobes are typically somewhat extended; see the AO density representations in Figure 6a. Both σ and π bonds can be formed due to the possibility of overlapping in different directions.

In the case of nonhybridized atomic orbitals, the orbital functions can be represented as a product $\varphi(r, \vartheta, \varphi) = R(r)Y(\vartheta, \varphi)$ of a radial factor $R(r)$ and an angular factor $Y(\vartheta, \varphi)$, where r, ϑ, φ are the polar coordinates with respect to the nucleus at the origin. One may then represent symbolically the topology of the orbital by “polar graphs” $r = |Y(\vartheta, \varphi)|$ or $r = |Y(\vartheta, \varphi)|^2$. In these cases, the symbolic lobes necessarily touch each other tangentially (Figure 6b). There is now no longer any direct relation between the (experimental or theoretical) orbital density distributions and these symbolic orbital pictures.

A further abstraction is found in many textbooks, where the lobes of the symbolic orbital pictures are represented slimmer still (Figure 6c) so that “metaphoric” pictures of molecular

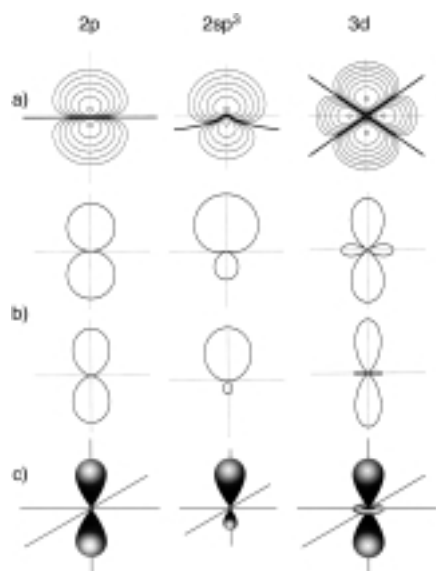


Figure 6. Plots and pictures of carbon 2p, carbon 2sp³, and chromium 3d orbitals. a) Contour plots, where the bold lines represent the zero contours; b) polar graphs (above: $r = |Y|$, below: $r = Y^2$); c) symbolic, textbook style, orbital pictures.

bonding can be generated in a transparent, non-overcrowded manner without explicitly showing the orbital overlaps, which are mandatory for covalent bonding. Of course, no experimental difference densities, independent of the choice of any reasonable reference densities, will resemble those textbook orbitals. Some textbook authors even call the latter orbital pictures (Figure 6c) “misleading”.

6. Closed-Shell Interactions

Closed-shell bonding is a controversial topic under active research for a number of years (see ref. [24]). Closed-shell atoms are distinguished by outer valence configurations of ns^2 , np^6 , or nd^{10} (for examples: ns^2 : He, Be, Ba, Au⁺; np^6 : O²⁻, Rb⁺, Xe; nd^{10} : Pd, Cu⁺, Au⁺). Four types of forces clarify closed-shell–closed-shell bonding: 1) the dispersion attraction $F \sim \alpha^2/R^6$ or $F \sim \nu^2/R^6$ (force F , internuclear distance R , and electric polarizabilities α , and atomic volumes ν of the two interacting atoms); 2) electrostatic effects, such as the ion-induced dipole attraction $F \sim \alpha/R^4$; 3) the common closed-shell repulsion (according to the Pauli exclusion principle), which acts as the electronic densities (with both spin directions) of different atoms begins to overlap; 4) specific overlapping orbital interference effects, which contribute to a lowering of the “Pauli repulsion” by hybridization of nearly degenerate orbitals such as 2s with 2p or 3d with 4s. In the case of point 4), the equilibrium interatomic distance may become rather short and the attractive forces (points 1) and, in the case of ions, 2)) become relatively large.

The weakest closed-shell–closed-shell attraction occurs in He₂, where α or ν are especially small and the minimum in the electronic potential-energy curve is just deep enough (calculated $D_e = -0.09$ kJ mol⁻¹ at $R_e = 3$ Å)^[25] to support the zero-vibrational level with dissociation energy D_0 as small as 10⁻⁵ kJ mol⁻¹.^[26] The (so far) strongest closed-shell attraction has been predicted to occur for an atomic–anionic system

with especially large α values, namely Ba–Au⁻ with a D_0 of about 140 kJ mol⁻¹.^[27]

An exciting, large class of substances is formed by clusters of Au^I molecular compounds such as A.^[28] These aurophilic systems exhibit Au⁺–Au⁺ closed-shell bond energies in the range 20–50 kJ mol⁻¹.^[24, 29] There exist two extreme viewpoints concerning the mechanism of the aurophilic attraction. The earlier, semiempirical calculations (by Hoffmann, Mingos, and Schmidbaur, among others^[30]) exaggerated the orbital stabilization of the nd^{10} – nd^{10} repulsive Pauli interaction on account of nd – $(n+1)s(p)$ hybridization and attributed the bonding to the lower energies of the bonding and antibonding d type MOs (Figure 2). The other point of view is that only the dispersion interaction (electron correlation) is responsible for Au^I–Au^I bonding.^[24] In this context, one may cite the s^2 – s^2 interaction in Be₂.^[31] Because of s – p hybridization, strong (Pauli-principle derived) repulsion between the two 2s² shells of Be occurs only at comparatively short distances, $R < 2$ Å. Although there is no bonding at all at the noncorrelated SCF MO level, the repulsion at $R > 2$ Å is weak enough to be compensated by the van der Waals attraction, which yields a potential curve minimum of $D_e = -10$ kJ mol⁻¹ at $R_e = 2.45$ Å.

A recent analysis of bonding in several Au^I cluster compounds^[32] indicates that, not unexpectedly, the synergetic cooperation of orbital interference and electron correlation is responsible for Au^I–Au^I bonding, too. We stress that such bonds are not characterized by pronounced “bond densities” between the atoms. This is expected, since electron correlation is an electron-pair phenomenon, which has only a small influence on the one-electron density distribution. Furthermore, Pauli repulsion (partially quenched by hybridization) is characterized by a slight reduction of electronic density in the overlap region.

7. Closed-Shell Cu–Cu Bonding in Cuprite?

A long time ago, O’Keeffe had calculated the Madelung constants and showed that the electrostatic interaction of the two point-charge lattices in Cu₂O is slightly repulsive.^[33] One obtains a value of the order 2 kJ mol⁻¹ for the effective charges mentioned in Section 2. While there exist several indications of a structural instability for the oxygen sublattice,^[34, 35] the Cu₄O₂ double lattice is still stable. Accordingly there must be either a topologically unexpected electronic-charge distribution in Cu₂O, with possibly far-reaching implications for high temperature superconductors, as postulated from time to time,^[5, 6a, 8] or the traditional dispersion and higher-order polarization effects are large enough (estimated to be a few kJ mol⁻¹) to overcome the electrostatic repulsion.

One may still speculate whether in addition some orbital interaction contributes to the stability of cuprite. In contrast to several experimental and theoretical investigations,^[9–11, 16] an older investigation by Fischer et al.^[8] and recently Zuo et al. “for the first time”,^[5] stated a significant electron difference density of about 0.2 e Å⁻³ over a volume of about 1 Å diameter in the center of the empty Cu₄ tetrahedra, containing about 0.1 e at each of the six 6d [$\frac{1}{4}\frac{1}{4}\frac{3}{4}$] D_{2d} positions.

The authors of the paper in *Nature*^[5] themselves believe that they have excluded all extinction, absorption, and other intensity errors, well known to be serious problems in cuprite studies.^[9] Neither statistical and possible systematic $\Delta\rho$ uncertainties are mentioned, nor uncertainties for the Wyck-off-6d position, which is expected to be especially sensitive. Another open question is whether an artifact of the theoretical refinement procedure has created the above-mentioned density feature. The Cu₄ hole is situated in a shortened octahedron of two axially positioned oxygen atoms (at 213 pm distance) and four equatorial ones (at 302 pm). At these distances, the single zeta basis used for the multipole refinement of the oxygen centers^[5] has appreciable density tails. Two other explanations for the Cu₄ density feature, however, may be ruled out: 1) due to oxygen atomic displacements in the percent range, this seems too large despite the exper-

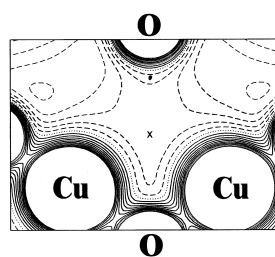


Figure 7. Electrostatic potential in the Cu₄ tetrahedron in cuprite. Note the flatness of the saddle in the center (*). Contour line values differ by 1 V; repulsive contours are dashed; zero potential is dotted. The Maddung potential is similarly flat and small in the central region.

imental indications of oxygen disorder,^[34] and 2) the presence of extra electrons in the matrix, due to oxygen deficiency, excess copper, or disproportionation of Cu⁺ into Cu²⁺ and e⁻.

The electrostatic potential inside the Cu₄ tetrahedra is rather flat with a plateau slightly repulsive due to the influence of the surrounding O²⁻ ions diminishing on proximity towards the Cu nuclei (Figure 7). Therefore, any additional electrons, according to our calculations,^[7] fill the holes in the Cu 3d shells and will not accumulate in the center of the Cu₄ tetrahedra.

For the defectless system, we calculate a positive difference density in a trigonally distorted diffuse belt around the Cu d¹⁰ shell, due to the d-s orbital hybridization, corresponding to the density deficiency on the orthogonal Cu-O axis. The local symmetry of Cu is D_{3d}, which is nicely reflected in the "Copper-Oxygen Bond" of ref. [5], although the diffuse belt is missing (see Figure 5b).

However, we do not find a pronounced density maximum but a minimum (in agreement with the band structure calculations of ref. [5]) at the center of Cu₄ and we do not find there more than a 0.045 e Å⁻³ difference density although we have included also an extended basis at the center (see Figures 3 and 4). A significant accumulation of electron density between the Cu⁺ cores will only occur at Cu-Cu distances of ≤ 2.5 Å, comparable to the ones in the Cu₂ molecule (222 pm) or in Cu metal (256 pm). As an example, we show the difference density of the calculated [CuF]₂ dimer **B** at different Cu-Cu distances in Figure 8. Upon decreasing the proximity to about 2.5 Å, the d-s hybridization density belts around copper do not remarkably influence each other; in cuprite, however, the Cu proximity is 3 Å.

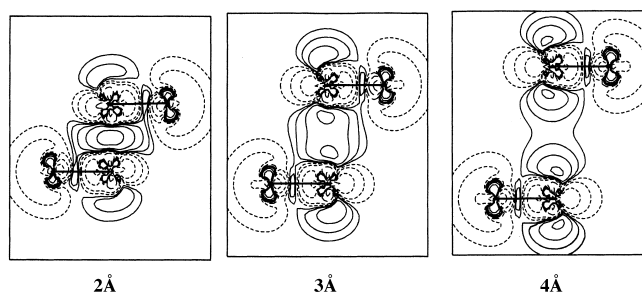
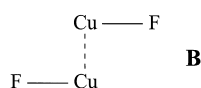


Figure 8. Electron density difference of calculated [CuF]₂ (structure **B**) with respect to Cu⁺ and F⁻ for Cu-Cu distances of 2–4 Å. Contour line values are $\pm 0.01 \times 2^n \text{ e Å}^{-3}$ ($n=0,1,2,\dots$); negative contour lines are dashed.

8. Conclusion

There seems as yet to exist no proof of significant Cu⁺-Cu⁺ closed-shell bonding at such large distances as found in cuprite, nor of a significant bonding (difference) density for Cu⁺-Cu⁺. No strongly founded doubts have arisen over the last decades against the chemical concept of a partially ionic covalency in Cu^I-O bonds. The effective charges are about one half of the formal ones, if one chooses the usual charge definitions. (Concerning the problematic choice of unit for the effective charges on atoms in molecules and crystals, see ref. [36]). There is about one half of an electron missing in the Cu d_z orbital, but about one electron is found in the 4sp shell of the formal Cu⁺ ion. There are many cases found in the literature, especially for transition metal compounds, where an appropriately defined difference electron density is dominated in some region of space by the difference between two atomic-orbital densities, or even by a single orbital density, if also the orbital densities are appropriately chosen. The symbolic textbook orbital plots are intrinsically different from orbital density-contour plots.

- [1] P. K. Feyerabend, *Against Method. Outline of an Anarchistic Theory of Knowledge*, Humanities Press, London, **1975**; P. K. Feyerabend, *Wider den Methodenzwang. Skizze einer anarchistischen Erkenntnistheorie*, Suhrkamp, Frankfurt/Main, **1976**.
- [2] K. R. Popper, *Logik der Forschung*, Springer, Wien, **1934/1935**; K. R. Popper, *The Logic of Scientific Discovery*, Hutchinson, London, **1959**.
- [3] A. Sokal, J. Bricmont, *Impostures Intellectuelles*, Odile Jacob, Paris, **1997**; A. Sokal, J. Bricmont, *Fashionable Nonsense*, Picador, New York, **1998**; A. Sokal, J. Bricmont, *Eleganter Unsinn*, Beck, München, **1999**; see also www.physics.nyu.edu/faculty/sokal.
- [4] T. S. Kuhn, *The Structure of Scientific Revolutions*, University Press, Chicago, **1962**; T. S. Kuhn, *Die Struktur wissenschaftlicher Revolutionen*, Suhrkamp, Frankfurt/Main, **1967**.
- [5] a) J. M. Zuo, M. Kim, M. O'Keeffe, J. C. H. Spence, *Nature* **1999**, *401*, 49; see also the authors' homepages and links therein and b) www.asu.edu/asunews/Releases/Cuprite.htm and c) <http://www.clasdean.la.asu.edu/news/cuprite.htm>.
- [6] a) C. J. Humphreys, *Nature* **1999**, *401*, 21; b) P. Yam, *Sci. Am.* **1999**, *281* (5), 28; K. Leutwyler, www.sciam.com/explorations/1999/092099 cuprite; c) P. Zurer, *Chem. Eng. News* **1999**, November 29, 38; d) A. G. Samuelson, *Curr. Sci. India* **1999**, *77*, 1131; e) *Phys. World* **1999**, October, 5; f) V. Drach, *Phys. Unserer Zeit* **1999**, *29*, 263; g) M. Rauner, *Phys. Bl.* **1999**, *55* (II), 17; h) S. Albus, *Nachr. Chem. Tech. Lab.* **1999**, *47*, 1298.
- [7] "A Theoretical Investigation of Cuprite": S. G. Wang, W. H. E. Schwarz, unpublished results.

- [8] a) D. Mullen, K. Fischer, *Z. Kristallogr.* **1981**, 156, 85; b) K. Eichhorn, J. Spilker, K. Fischer, *Acta Crystallogr. Sect. A* **1984**, 40, C160.
- [9] R. Restori, D. Schwarzenbach, *Acta Crystallogr. Sect. B* **1986**, 42, 201.
- [10] a) A. Kirfel, K. Eichhorn, *Acta Crystallogr. Sect. A* **1990**, 46, 271; b) A. Kirfel, H. G. Krane (Hamburger Synchrotronstrahlungslabor/Deutsches Elektronen-Synchrotron), *HASYLAB/DESY Annual Report*, **1999**.
- [11] a) T. Lippmann, J. R. Schneider, *J. Appl. Crystallogr.* **2000**, 33, in press; b) T. Lippmann, J. R. Schneider, *HASYLAB/DESY Annual Report*, **1998**; www-hasyllab.desy.de/science/annual_reports/1998/part1/contrib/24/1298.pdf.
- [12] a) R. D. Shannon, *Acta Crystallogr. Sect. A* **1976**, 32, 751; b) R. D. Shannon, *Struct. Bonding Cryst.* **1981**, 2, 53.
- [13] a) L. Pauling, *J. Am. Chem. Soc.* **1932**, 54, 3570; b) L. Pauling, *The Nature of the Chemical Bond*, Cornell University Press, Ithaca, NY, **1939**; L. Pauling, *Die Natur der Chemischen Bindung*, Verlag Chemie, Weinheim, **1962**; c) R. T. Sanderson, *Polar Covalence*, Academic Press, New York, **1983**.
- [14] P. Coppens, *X-Ray Charge Densities and Chemical Bonding*, Oxford University Press, Oxford, **1997**; V. G. Tsirelson, R. P. Ozerov, *Electron Density and Bonding in Crystals*, Institute of Physics, Bristol, **1996**.
- [15] M. A. Spackman, *Annu. Rep. Prog. Chem. C* **1997**, 94, 177; M. A. Spackman, *Annu. Rep. Prog. Chem. C* **1994**, 91, 175.
- [16] P. Marksteiner, P. Blaha, K. Schwarz, *Z. Phys. B* **1986**, 64, 119.
- [17] M. S. Liao, W. H. E. Schwarz, *Acta Crystallogr. Sect. B* **1994**, 50, 9.
- [18] L. E. Orgel, *J. Chem. Soc.* **1958**, 4186.
- [19] M. S. Liao, W. H. E. Schwarz, *J. Alloys Compd.* **1997**, 246, 2.
- [20] W. H. E. Schwarz, B. Müller, *Chem. Phys. Lett.* **1990**, 166, 621; W. H. E. Schwarz, A. Langenbach, L. Birlenbach, *Theor. Chim. Acta* **1994**, 88, 233, and references therein.
- [21] S. G. Wang, W. H. E. Schwarz, *J. Chem. Phys.* **1996**, 105, 4641.
- [22] B. Rees, *Acta Crystallogr. Sect. A* **1976**, 32, 48.
- [23] N. Rösch, *Chem. Phys.* **1983**, 80, 1.
- [24] P. Pykkö, *Chem. Rev.* **1997**, 97, 597; *Unkonventionelle Wechselwirkungen in der Chemie metallischer Elemente* (Ed.: B. Krebs), VCH, Weinheim, **1992**.
- [25] T. Van Mourik, T. H. Dunning, *J. Chem. Phys.* **1999**, 111, 9248, and references therein.
- [26] F. Luo, G. C. McBane, G. Kim, C. F. Giese, W. R. Gentry, *J. Chem. Phys.* **1993**, 98, 3564; T. Korona, H. L. Williams, R. Bukowski, B. Jeziorski, K. Szalewicz, *J. Chem. Phys.* **1997**, 106, 5109.
- [27] R. Wesendrup, P. Schwerdtfeger, *Angew. Chem.* **2000**, 112, 938; *Angew. Chem. Int. Ed.* **2000**, 39, 907.
- [28] P. Pykkö, Y. F. Zhao, *Angew. Chem.* **1991**, 103, 622; *Angew. Chem. Int. Ed. Engl.* **1991**, 30, 604; O. D. Häberlen, N. Rösch, *J. Phys. Chem.* **1993**, 97, 4970.
- [29] H. Schmidbaur, *Chem. Soc. Rev.* **1995**, 391.
- [30] A. Dedieu, R. Hoffmann, *J. Am. Chem. Soc.* **1978**, 100, 2074; R. Hoffmann, *Angew. Chem.* **1982**, 94, 725; *Angew. Chem. Int. Ed. Engl.* **1982**, 21, 711; K. P. Hall, D. M. P. Mingos, *Prog. Inorg. Chem.* **1984**, 32, 237; D. G. Evans, D. M. P. Mingos, *J. Organomet. Chem.* **1985**, 295, 389; A. Görling, N. Rösch, D. E. Ellis, H. Schmidbaur, *Inorg. Chem.* **1991**, 30, 3986.
- [31] For example, C. Sosa, J. Noga, R. J. Bartlett, *J. Chem. Phys.* **1988**, 88, 5974.
- [32] "On the Aurophilic Interaction": S. G. Wang, W. H. E. Schwarz, unpublished results.
- [33] M. O'Keeffe, *J. Chem. Phys.* **1963**, 38, 3035.
- [34] M. Ivanda, D. Waasmaier, A. Endriss, J. Ihringer, A. Kirfel, W. Kiefer, *J. Raman Spectrosc.* **1997**, 28, 487; reference [10a].
- [35] J. Hallberg, R. C. Hanson, *Phys. Status Solidi* **1970**, 42, 305.
- [36] J. Meister, W. H. E. Schwarz, *J. Phys. Chem.* **1994**, 98, 8245.